

Experimental Investigation of Surface Integrity and Machining Characteristics of Ti–6Al–4V Alloy Machined by Wire-EDM Process



Sandeep Malik and Vineet Singla

1 Introduction

Titanium–Aluminium–Vanadium-based biomedical alloy (Ti–6Al–4V) was widely and commercially used biomaterial for medical applications like development of implants, screws, and plates, etc., owing to its desirable biocompatibility and excellent biomechanical properties [1]. This particular grade of titanium (Ti) has been regarded as “wonder metal” as it possesses very low density and its strength could be enhanced, enormously, by using different types of alloying elements, which include tin, aluminum, chromium, manganese, vanadium, and molybdenum, etc. [2]. However, it has been classified as the “hard-to-cut” category of the materials, which means it is extremely difficult to machine Ti as results of its low thermal conductivity, elastic modulus, and high chemical reactivity [3]. The limited thermal conductivity of Ti restricts the distribution of the heat from the machining interface and causes high tool abrasive, adhesive, and diffusive wear mechanisms which further lead to catastrophic tool failures.

Likewise, during machining the obtainable surface finish is degraded by a small degree of elastic modulus. In addition, high chemical reactivity, especially at high temperatures, increases the adhesion between the tool and the workpiece and results in the cutting tool’s wear/failure [4, 5]. Therefore, it has been observed that the efficacy of conventional machining methods for processing Ti alloys is marginal and, further, the potential of nonconventional machining methods, such as electric discharge machining (EDM), ultrasonic machining, magnetic abrasive machining, etc., could be explored. Reportedly, in case of EDM process, the material removal mechanism is governed by the rapid and repetitive spark discharges across the gap between electrode and workpiece [6]. Basically, EDM is a process of electrothermal machining that produces a large number of electrical sparks in a fraction of seconds,

S. Malik (✉) · V. Singla

Department of Mechanical Engineering, UIET, Maharshi Dayanand University, Rohtak, Haryana, India

e-mail: sandymalik0077@gmail.com

© Springer Nature Singapore Pte Ltd. 2020

S. Singh et al. (eds.), *Advances in Materials Processing*, Lecture Notes

in Mechanical Engineering, https://doi.org/10.1007/978-981-15-4748-5_14

resulting in intense heat energy that is sufficient to remove the working material [7]. In addition, EDM could be used for electrically conductive materials irrespective of their hardness and strength. Prakash et al. have highlighted the potential of machining Ti-based alloy by using EDM process, for biomedical applications [8]. Previous investigations reported that EDM modifies the surface of Ti–6Al–4V alloy in order to yield a biocompatible coating of nanohydrides [9]. This is, in fact, mainly due to the electrothermal nature of the EDM system, the simultaneous action of thermal energy generation and process cycle quenching [10]. It affects the process and a variety of morphological disorders are usually developed on the machined surface, such as surface roughness, cracks, and pit/dimples that deteriorate the surface value [11, 12]. However, during the actual work scenario, the resulted morphological defects degrade the corrosion performance [13], and fatigue performance [14] of biomedical device.

Therefore, in order to overcome the above-mentioned disorders, number of advancements in EDM process has been suggested in the literature, such as wire-cut EDM [15], vibration assistance during EDM [16], rotational EDM [17], HyFlex™ EDM [18], coating of EDM tool [19], dry EDM [20], and powder mixed slurry EDM [21–28]. Rahman et al. outlined the morphological, chemical, and crystallographic characteristics of recast layer on wire-cut EDM processed Ti–6Al–4V alloy [29]. Kuriachen et al. studied tribological performance of wire-cut EDM surface and found an increase in the oxide layer formation that improved the tribological properties [30]. Similarly, other studies emphasized on the machining of magnesium (Mg) alloys by wire-cut EDM process [31, 32]. Wire-cut EDM showed excellent attributes toward the cell viability [33, 34].

Overall, it has been reviewed that a very limited research studies have been reported on machining/cutting of microholes in Ti–6Al–4V alloy, focusing biomedical applications. So, the scope of machining of Ti–6Al–4V alloy and investigating the obtainable surface and machining characteristics is huge with regards to wire-cut EDM process. The present study is focused perform an investigation onto the effect of wire-cut EDM (W-EDM) process parameters in response of the surface morphology, surface chemistry, and machining characteristics.

2 Materials and Method

The workpiece material is Ti–6Al–4V alloy as rectangular plate with dimensions as 15 mm × 10 mm × 50 mm. Experiments were performed using an Electronoca wire-electrical discharge machine (W-EDM) as shown in Fig. 1. Distilled water was used as the dielectric fluid in this experiment. The material removal rate (MRR) was calculated for all the included experimental runs, as suggested by design of experimentation, by observing the average amount of material removed with respect to the incurred cutting time. Further, surface roughness (SR) of the machined work samples has been recorded by using surface roughness tester (Talysurf: Mitutoyo). The selected input process parameters and their levels are given in Table 1.



Fig. 1 Schematic representation of WEDM machine

Table 1 Process parameters and their levels

| Process parameters | Units | Parameter designation | Levels | | |
|--------------------|---------|-----------------------|--------|-----|-----|
| | | | L-1 | L-2 | L-3 |
| Peak current | amp | I_p | 80 | 120 | 160 |
| Pulse duration | μs | T_{on} | 100 | 150 | 200 |
| Pulse interval | μs | T_{off} | 50 | 100 | 150 |
| Wire feed | mm/s | Wf | 6 | 8 | 10 |

Taguchi-based design of experimental (DOE) technique is used to get information about interaction and main effects of parameters for experiments. The main objective of Taguchi design is to get best possible results with minimum variation. The statically design of the experimentation, design of experiment (DOE), has

been proved for providing best combination of the input parametric levels at minimum cost and time consumption. MINITAB-16-based statistical software package, as commercially available, has been employed for managing the raw data and to convert the same into responses, signal/noise (S/N) plots, and interaction plots. Here, MRR and SR have been processed at “larger the better” and “smaller the better” settings. The observed results in accordance of Taguchi L-27 orthogonal array are shown in Table 2.

3 Results and Discussion

3.1 Analysis of MRR

From Fig. 2, it has been seen that the MRR increased with peak current (I_p), mainly because of the fact that at higher level of I_p a large amount of heat is enlightened at the cutting interface and finally traveled into the workpiece. Owing to this, the size and shape of pits/craters on the machined surface increased, and finally affected the MRR. Specifically, the MRR value increased from 1.82 to 2.3 mm³/min as the level of the I_p increased from 80 to 160 A. Further, it has been observed that the MRR value also increased with the pulse duration. This is because of the proportionality of discharge energy and pulse duration that helped machining process in enlarging the craters [21]. In this case, the MRR value enhanced from 1.85 to 2.35 mm³/min as the pulse duration increased from 100 to 200 μ s. The MRR value increased from 1.75 to 2.27 mm³/min, when pulse interval increased from 25 to 75 μ s. The MRR decreases with wire feed and increased with gap voltage. These two parameters have a very less effect on the MRR. Figure 3 shows the effect of interactions of parameters on MRR. It can be clearly seen that interaction of parameters has large and high impact on the MRR. The MRR increased in higher proposition when peak current increased combination with pulse duration and pulse interval.

Overall, the best parametric setting suggested by Taguchi is peak current (A3), pulse duration (B3), duty cycle (C3), and spark gap (E3), and low value of wire feed rate (D1). Table 3, analysis of variance (ANOVA), highlighted that the peak current, pulse-on, and pulse-off time have a significant contribution toward increasing the MRR.

3.2 Analysis of SR

From the Fig. 4, It was noticed that the SR increased with peak current (I_p), as when the I_p was increased, an immense amount of heat was illuminated and sunk into the workpiece. As a result, on the regenerated layer, the pits/craters increased, which increased the SR further. The pulse duration increased the SR value. This may be

Table 2 Process parameters and their levels

| Sr. no. | I_p | T_{on} | T_{off} | F_d | V | Mean | | S/N ratio | |
|---------|-------|----------|-----------|-------|-----|-------|-------|-----------|--------|
| | | | | | | MRR | SR | MRR | SR |
| 1 | 80 | 100 | 50 | 6 | 25 | 1.240 | 0.890 | 1.868 | 1.013 |
| 2 | 80 | 100 | 100 | 8 | 50 | 1.760 | 1.029 | 4.910 | -0.251 |
| 3 | 80 | 100 | 150 | 10 | 75 | 2.286 | 1.155 | 7.182 | -1.250 |
| 4 | 80 | 150 | 50 | 8 | 75 | 1.734 | 0.998 | 4.781 | 0.017 |
| 5 | 80 | 150 | 100 | 10 | 25 | 2.000 | 1.079 | 6.021 | -0.661 |
| 6 | 80 | 150 | 150 | 6 | 50 | 1.780 | 1.022 | 5.008 | -0.186 |
| 7 | 80 | 200 | 50 | 10 | 50 | 1.874 | 1.059 | 5.455 | -0.500 |
| 8 | 80 | 200 | 100 | 6 | 75 | 1.314 | 0.910 | 2.372 | 0.822 |
| 9 | 80 | 200 | 150 | 8 | 25 | 2.274 | 1.166 | 7.136 | -1.337 |
| 10 | 120 | 100 | 50 | 6 | 25 | 1.240 | 0.873 | 1.868 | 1.179 |
| 11 | 120 | 100 | 100 | 8 | 50 | 2.514 | 1.198 | 8.007 | -1.568 |
| 12 | 120 | 100 | 150 | 10 | 75 | 1.874 | 1.063 | 5.455 | -0.529 |
| 13 | 120 | 150 | 50 | 8 | 75 | 1.894 | 1.044 | 5.548 | -0.375 |
| 14 | 120 | 150 | 100 | 10 | 25 | 2.760 | 1.262 | 8.818 | -2.019 |
| 15 | 120 | 150 | 150 | 6 | 50 | 1.834 | 1.046 | 5.268 | -0.388 |
| 16 | 120 | 200 | 50 | 10 | 50 | 1.906 | 1.059 | 5.602 | -0.495 |
| 17 | 120 | 200 | 100 | 6 | 75 | 2.726 | 1.342 | 8.711 | -2.555 |
| 18 | 120 | 200 | 150 | 8 | 25 | 2.660 | 1.280 | 8.498 | -2.147 |
| 19 | 160 | 100 | 50 | 6 | 25 | 2.146 | 1.124 | 6.633 | -1.012 |
| 20 | 160 | 100 | 100 | 8 | 50 | 1.560 | 0.957 | 3.862 | 0.380 |

(continued)

Table 2 (continued)

| Sr. no. | I_p | T_{on} | T_{off} | F_d | V | Mean | | S/N ratio | |
|---------|-------|----------|-----------|-------|-----|-------|-------|-----------|--------|
| | | | | | | MRR | SR | MRR | SR |
| 21 | 160 | 100 | 150 | 10 | 75 | 1.914 | 1.060 | 5.639 | -0.507 |
| 22 | 160 | 150 | 50 | 8 | 75 | 1.714 | 0.998 | 4.680 | 0.017 |
| 23 | 160 | 150 | 100 | 10 | 25 | 1.714 | 0.994 | 4.680 | 0.054 |
| 24 | 160 | 150 | 150 | 6 | 50 | 3.274 | 1.434 | 10.302 | -3.133 |
| 25 | 160 | 200 | 50 | 10 | 50 | 2.074 | 1.114 | 6.336 | -0.935 |
| 26 | 160 | 200 | 100 | 6 | 75 | 3.526 | 1.446 | 10.946 | -3.201 |
| 27 | 160 | 200 | 150 | 8 | 25 | 2.394 | 1.202 | 7.582 | -1.598 |

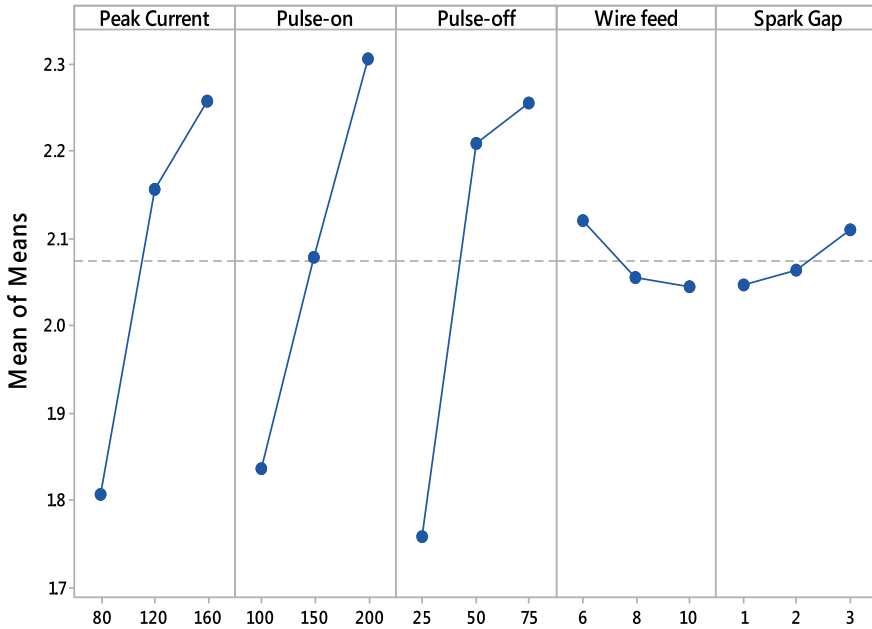


Fig. 2 Main effects plot of MRR

because discharge energy is a pulse duration feature that increases crater depth and width [21]. It is recorded that the SR value grew from 1,027 to 1,178 μm as the length of the pulse increased from 100 to 200 μs . The SR increases with the pulse interval because the discharge debris had sufficient time to flush out the machining with the increase in the pulse interval zone. The SR decreases with wire feed and increased with gap voltage. These two parameters have very least effect on the SR. Figure 5 shows the effect of interactions of parameters on SR. It can be clearly seen that interaction of parameters has large and high impact on the SR. The SR increased in higher proposition when peak current increased combination with pulse duration and pulse interval. The best parametric setting suggested by Taguchi is peak current (A3), pulse duration (B3), duty cycle (C3), spark gap (E1), wire feed rate (D3). Table 4 highlighted that all the input process parameters, in case of SR, have significant contribution toward increasing the SR except wire feed and spark gap. These two parameters were, therefore, pooled form the analysis.

3.3 Surface Morphology Analysis

Machined surface morphology investigation was conducted to evaluate the surface quality obtained through the WEDM process. Three samples were chosen for machined surface morphology investigation (Sample at low peak current, sample at

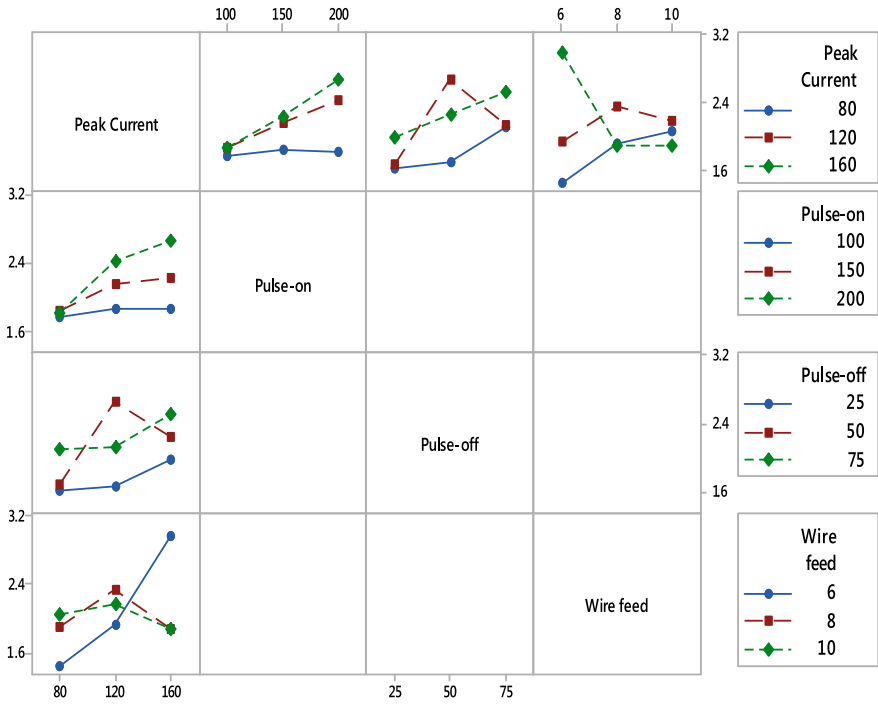


Fig. 3 Interaction effects plot of MRR

Table 3 Analysis of variance for MRR

| Source | DF | Seq-SS | Adj-SS | Adj-MS | F | P | % |
|------------------------|----|--------|--------|--------|--------|-------|-------|
| Peak current | 2 | 1.006 | 1.006 | 0.503 | 12.640 | 0.019 | 0.123 |
| Pulse-on | 2 | 0.987 | 0.987 | 0.493 | 12.400 | 0.019 | 0.120 |
| Pulse-off | 2 | 1.354 | 1.354 | 0.677 | 17.010 | 0.011 | 0.165 |
| Wire feed | 2 | 0.030 | 0.030 | 0.015 | 0.370 | 0.710 | 0.004 |
| Spark gap | 2 | 0.018 | 0.018 | 0.009 | 0.230 | 0.805 | 0.002 |
| Peak current*Pulse-on | 4 | 0.426 | 0.426 | 0.107 | 2.680 | 0.182 | 0.052 |
| Peak current*pulse-off | 4 | 0.996 | 0.996 | 0.249 | 6.260 | 0.042 | 0.121 |
| Peak current*wire feed | 4 | 3.220 | 3.220 | 0.805 | 20.230 | 0.006 | 0.393 |
| Residual error | 4 | 0.159 | 0.159 | 0.040 | | | 0.019 |
| Total | 26 | 8.196 | | | | | |

* mean “x” (Multiplication)

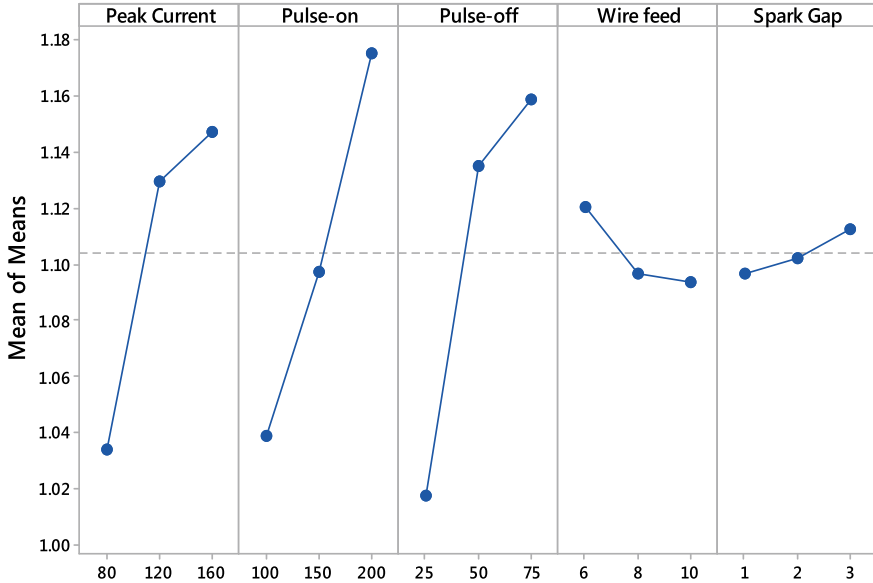


Fig. 4 Main effects plot of SR

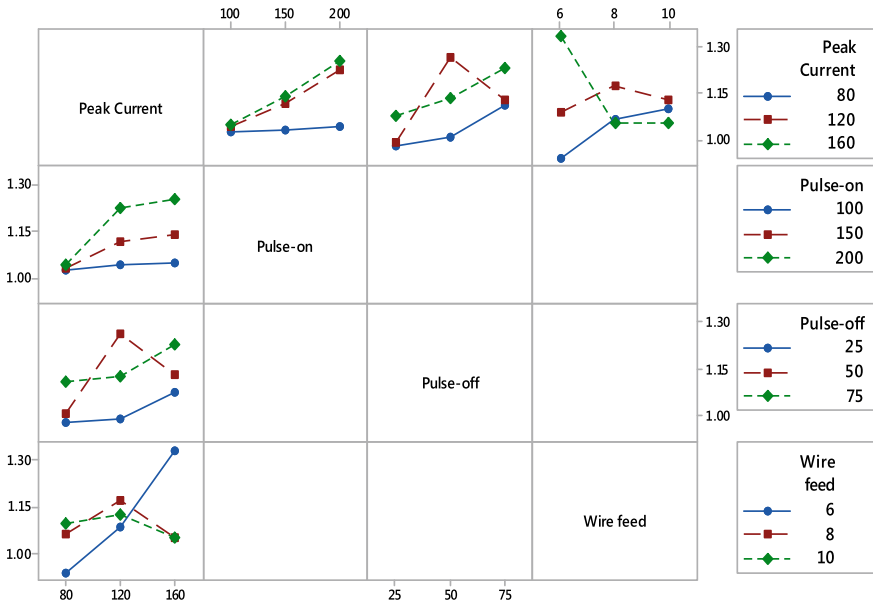


Fig. 5 Interaction effects plot of SR

Table 4 Analysis of variance for SR

| Source | DF | Seq-SS | Adj-SS | Adj-MS | <i>F</i> | <i>P</i> | % |
|------------------------|----|--------|--------|--------|----------|----------|-------|
| Peak current | 2 | 1.006 | 1.006 | 0.503 | 12.640 | 0.019 | 0.123 |
| Pulse-on | 2 | 0.987 | 0.987 | 0.493 | 12.400 | 0.019 | 0.120 |
| Pulse-off | 2 | 1.354 | 1.354 | 0.677 | 17.010 | 0.011 | 0.165 |
| Wire feed | 2 | 0.030 | 0.030 | 0.015 | 0.370 | 0.710 | 0.004 |
| Spark gap | 2 | 0.018 | 0.018 | 0.009 | 0.230 | 0.805 | 0.002 |
| Peak current*pulse-on | 4 | 0.426 | 0.426 | 0.107 | 2.680 | 0.182 | 0.052 |
| Peak current*pulse-off | 4 | 0.996 | 0.996 | 0.249 | 6.260 | 0.052 | 0.121 |
| Peak current*wire feed | 4 | 3.220 | 3.220 | 0.805 | 20.230 | 0.006 | 0.393 |
| Residual error | 4 | 0.159 | 0.159 | 0.040 | | | 0.019 |
| Total | 26 | 8.196 | | | | | |

* mean "x" (Multiplication)

moderate peak current, and sample at high peak current). It can be clearly seen that at low peak current (80 A), the surface was very smooth and low degree of craters were found. Only scars during cutting due to wire travel were observed, as can be seen in Fig. 6a. The associated EDS spectrum of machined surface presents the significant availability of base material elements along with high content on oxygen (O) element, as can be seen in Fig. 6b. The element O reacts with Ti and formed rutile TiO_2 , which is beneficial for the corrosion resistance and bioactivity. When the peak current was increased to 120 A, the machined surface become rough and craters were observed on the surface, as can be seen in Fig. 6c. The associated EDS spectrum of machined surface presents the significant availability of base material elements along with high content on oxygen (O) element, as can be seen in Fig. 6d. When the peak current was increased to 160 A, highly rough surface was observed. Deep and wide craters were formed on the machined surface results in poor surface finish and surface quality, as can be seen in Fig. 6e. The associated EDS spectrum of machined surface presents the significant availability of base material elements along with high content on oxygen (O) element, as can be seen in Fig. 6f. As the peak current increased the O content in the machined surface morphology increased, which increased the formation of formed rutile TiO_2 . Thus results in good surface quality in terms of bioactivity.

4 Conclusions

Following conclusions could be drawn from this investigation:

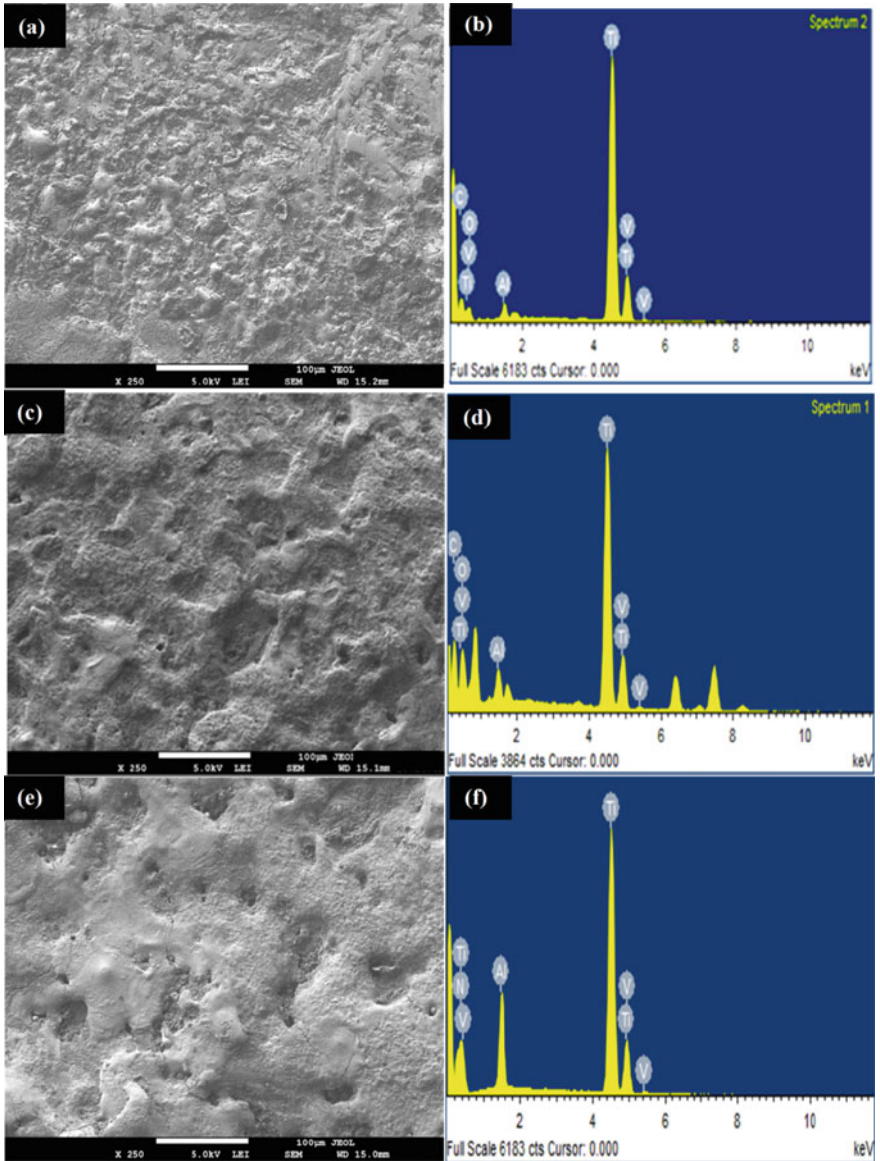


Fig. 6 Surface morphology of Ti-6Al-4V alloy by W-EDM process at different peak current levels: **a** 80 A, **b** 120 A, and **c** 180 A

- From the Taguchi-based design of experimentation, it has been found that peak current, pulse-on and pulse-off times have significantly affected the obtained MRR and SR results. In case of MRR, the optimized process parametric setting is A3, B3, C3, D1, and E3. The maximum MRR was obtained 3.69 mm³/min, whereas in case of SR, the optimized process parametric setting is A1, B1, C1, D3, and E1. The maximum SR was obtained 1.02 μm.
- The machined surface morphology depicts that rutile TiO₂ were formed, which is beneficial to enhance the corrosion resistance and bioactivity of implant.
- From the present investigations, it can be concluded that W-EDM can be used as potential nonconventional machining/cutting technique to implants processing.

References

1. T Zaman, H.A., Safian, S., Idris, M.H., Kamarudin, A.: Metallic biomaterial for medical implant applications: a review. *Appl. Mech. Mater.* **735**, 19–25 (2015). www.scientific.net/AMM.735.19
2. Niinomi, M., Narushima, T., Naka, M. *Advances in Metallic Biomaterials*, p. 348. Springer Berlin Heidelberg, Berlin, Germany (2015)
3. Pramanik, A.: Problems and solutions in machining of titanium alloys. *Int. J. Adv. Manuf. Technol.* **70**(5), 919–928 (2014). <https://doi.org/10.1007/s00170-013-5326-x>
4. Klocke, F., Zeis, M., Klink, A., Veselovac, D.: Technological and economical comparison of roughing strategies via milling, EDM and ECM for titanium-and nickel-based blisks. *Procedia CIRP* **2**(1), 98–101 (2012). <https://doi.org/10.1016/j.cirpj.2013.02.008>
5. Andrew Y.C. Nee.: *Handbook of Manufacturing Engineering and Technology*, 3485 pp. Springer, London (2015)
6. Kumar, S.; Singh, R.; Batish, A.; Singh, T.P. Electric discharge machining of titanium and its alloys: a review. *Int. J. Mach. Mach. Mater.* **11**(1), 84–111 (2012). <https://doi.org/10.1504/ijmmm.2012.044922>
7. Prakash, C., Kansal, H.K., Pabla, B.S., Puri, S.: Experimental investigations in powder mixed electric discharge machining of Ti–35Nb–7Ta–5Zrβ-titanium alloy. *Mater. Manuf. Processes* **32**(3), 274–285 (2017)
8. Prakash, C., Kansal, H.K., Pabla, B.S., Puri, S., Aggarwal, A.: Electric discharge machining—a potential choice for surface modification of metallic implants for orthopedic applications: A review. *Proc. Inst. Mech. Eng. Part B: J. Eng. Manuf.* **230**(2), 331–353 (2016)
9. Peng, P.W., Ou, K.L., Lin, H.C., Pan, Y.N., Wang, C.H.: Effect of electrical-discharging on formation of nanoporous biocompatible layer on titanium. *J. Alloy. Compd.* **492**(1–2), 625–630 (2010). <https://doi.org/10.1016/j.jallcom.2009.11.197>
10. Yang, T.S., Huang, M.S., Wang, M.S., Lin, M.H., Tsai, M.Y., Wang, P.Y.: Effect of electrical discharging on formation of nanoporous biocompatible layer on Ti-6Al-4V alloys. *Implant dentistry* **22**(4), 374–379 (2013). <https://doi.org/10.1097/ID.0b013e31829a170a>
11. Bin, T.C., Xin, L.D., Zhan, W., Yang, G.: Electro-spark alloying using graphite electrode on titanium alloy surface for biomedical applications. *Appl. Surf. Sci.* **257**(15), 6364–6371 (2011). <https://doi.org/10.1016/j.apsusc.2011.01.120>
12. Harcuba, P., Bačakova, L., Strasky, J., Bačakova, M., Novotna, K., Janeček, M.: Surface treatment by electric discharge machining of Ti–6Al–4V alloy for potential application in orthopaedics. *J. Mech. Behav. Biomed. Mater.* **7**, 96–105 (2012). <https://doi.org/10.1016/j.jmbbm.2011.07.001>

13. Janecek, M., Novy, F., Strasky, J., Harcuba, P., Wagner, L.: Fatigue endurance of Ti-6Al-4V alloy with electro-eroded surface for improved bone in-growth. *J. Mech. Behav. Biomed. Mater.* **4**, 417–422 (2011). <https://doi.org/10.1016/j.jmbbm.2010.12.001>
14. Strasky, J., Janecek, M., Harcuba, P., et al.: The effect of microstructure on fatigue performance of Ti-6Al-4V alloy after EDM surface treatment for application in orthopaedics. *J. Mech. Behav. Biomed. Mater.* **4**, 1955–1962 (2011). <https://doi.org/10.1016/j.jmbbm.2011.06.012>
15. Goswami, A., Kumar, J.: Optimization in wire-cut EDM of nimonic-80A using Taguchi's approach and utility concept. *Eng. Sci. Technol. Int. J.* **17**(4), 236–246 (2014)
16. Shabgard, M.R., Alenabi, H.: Ultrasonic assisted electrical discharge machining of Ti-6Al-4V alloy. *Mater. Manuf. Processes* **30**(8), 991–1000 (2015). <https://doi.org/10.1080/10426914.2015.1004686>
17. Dwivedi, A.P., Choudhury, S.K.: Effect of tool rotation on MRR, TWR and surface integrity of AISI-D3 steel using rotary EDM process. *Mater. Manuf. Processes* (2016). <https://doi.org/10.1080/10426914.2016.1140198>
18. Pirani, C., Iacono, F., Generali, L., Sassatelli, P., Nucci, C., Lusvardi, L., Gandolfi, M.G., Prati, C.: HyFlex EDM: superficial features, metallurgical analysis and fatigue resistance of innovative electro discharge machined NiTi rotary instruments. *Int. Endod. J.* (2015). <https://doi.org/10.1111/iej.12470>
19. Krishna, M.E., Patowari, P.K.: Parametric study of electric discharge coating using powder metallurgical green compact electrodes. *Mater. Manuf. Processes* **29**(9), 1131–1138 (2014). <https://doi.org/10.1080/10426914.2014.930887>
20. Dhakar, K., Dvivedi, A.: Parametric Evaluation on near-dry electric discharge machining. *Mater. Manuf. Processes* **31**(4), 413–421 (2016)
21. Prakash, C., Kansal, H.K., Pabla, B.S., Puri, S.: Processing and characterization of novel biomimetic nanoporous bioceramic surface on β -Ti implant by powder mixed electric discharge machining. *J. Mater. Eng. Perform.* (2015). <https://doi.org/10.1007/s11665-015-1619-6>
22. Chander Prakash, Sunpreet Singh, Pabla, B.S.: Multi-objective optimization of EDM parameters to deposit HA-containing coating on Mg-Zn-Mn alloy using particle swarm optimization. *Vacuum* **158**, 180–190 (2018)
23. Chander Prakash, Sunpreet Singh, Pabla, B.S., Uddin, M.S.: Synthesis, characterization, corrosion and bioactivity investigation of nano-HA coating deposited on biodegradable Mg-Zn-Mn alloy. *Surf. Coat. Technol.* **346**, 9–18 (2018)
24. Chander Prakash and M. S. Uddin, "Surface modification of β -phase Ti implant by hydroxyapatite mixed electric discharge machining to enhance the corrosion resistance and in-vitro bioactivity. *Surf. Coat. Technol. Part A* **236**, 134–145 (2017)
25. Chander Prakash, Kansal, H.K., Pabla, B.S., Sanjeev Puri: Effect of surface nano-porosities fabricated by powder mixed electric discharge machining on bone-implant interface: an experimental and finite element study. *Nanosci. Nanotechnol. Lett.* **8**(10), 815–826 (2016). <https://doi.org/10.1166/nnl.2016.2255>
26. Chander Prakash, Kansal, H.K., Pabla, B.S., Sanjeev Puri: Multi-objective optimization of powder mixed electric discharge machining parameters for fabrication of biocompatible layer on β -Ti alloy using NSGA-II coupled with Taguchi based response surface methodology. *J. Mech. Sci. Technol.* **30**(9), 4195–4204 (2016). <https://doi.org/10.1007/s12206-016-0831-0>
27. Chander Prakash, H.K. Kansal, B.S. Pabla, and Sanjeev Puri: Powder mixed electric discharge machining an innovative surface modification technique to enhance fatigue performance and bioactivity of β -Ti implant for orthopaedics application. *J. Comput. Inf. Sci. Eng.* **14**(4), 1–9, 2016. <https://doi.org/10.1115/1.4033901>
28. Chander Prakash, H.K. Kansal, B.S., Sanjeev Puri: Potential of powder mixed electric discharge machining to enhance the wear and tribological performance of β -Ti implant for orthopedic applications. *J. Nanoeng. Nanomanuf.* **5**(4), 261–269 (2015)
29. Kuriachen, B., Lijesh, K.P. and Kuppan, P.: Multi response optimization and experimental investigations into the impact of wire EDM on the tribological properties of Ti-6Al-4V. *Trans. Indian Inst. Met.*, 1–11 (2018)

30. Rahman, S.S., Ashraf, M.Z.I., Bashar, M.S., Kamruzzaman, M., Amin, A.N., Hossain, M.M.: Crystallinity, surface morphology, and chemical composition of the recast layer and rutile-TiO₂ formation on Ti-6Al-4V ELI by wire-EDM to enhance biocompatibility. *Int. J. Adv. Manuf. Technol.* **93**(9–12), 3285–3296 (2017)
31. Klocke, F., Schwade, M., Klink, A., Kopp, A.: EDM machining capabilities of magnesium (Mg) alloy WE43 for medical applications. *Procedia Eng.* **19**, 190–195 (2011). <https://doi.org/10.1016/j.proeng.2011.11.100>
32. Razak, M.A., Abdul-Rani, A.M.; Rao, T.V.V.L.N., Pedapati, S.R., Kamal, S.: Electrical discharge machining on biodegradable AZ31 magnesium alloy using taguchi method. *Procedia Eng.* **148**, 916–922 (2016). <https://doi.org/10.1016/j.proeng.2016.06.501>
33. Klocke, F., Schwade, M., Klink, A., Kopp, A.: Influence of electro discharge machining of biodegradable magnesium on the biocompatibility. *Procedia CIRP* **5**, 88–93 (2013). <https://doi.org/10.1016/j.procir.2013.01.018>
34. Ponappa, K., Aravindan, S., Rao, P.V., Ramkumar, J., Gupta, M.: The effect of process parameters on machining of magnesium nano alumina composites through EDM. *Int. J. Adv. Manuf. Technol.* **46**, 1035–1042 (2010). <https://doi.org/10.1007/s00170-009-2158-9>